

Transverse single-spin asymmetry in the low-virtuality leptoproduction of open charm as a probe of the gluon Sivers function

Rohini M. Godbole,^{1,*} Abhiram Kaushik,^{1,†} and Anuradha Misra^{2,‡}

¹*Centre for High Energy Physics, Indian Institute of Science, Bangalore, India.*

²*Department of Physics, University of Mumbai, Mumbai, India.*

(Dated: December 14, 2024)

Abstract

We study the low-virtuality inclusive leptoproduction of open charm, $p^\uparrow l \rightarrow D^0 + X$, treated here in a generalized parton model framework, as a probe of the gluon Sivers function. At leading order, this process is sensitive only to the gluon content of the proton. Hence any detection of a transverse single-spin asymmetry in this process would be clear indication of a non-zero gluon Sivers function. Considering COMPASS and a future Electron-Ion Collider, we present predictions for asymmetry using fits of the GSF available in literature. Predictions for peak asymmetry values lie in the range of 0.8% to 12%. We also present estimates of the upper bound on the asymmetry as obtained with a maximal gluon Sivers function. Further, for the case of the Electron-Ion Collider, we evaluate the asymmetry in the muons decaying from the D -meson and find that the asymmetry is well preserved in the kinematics of the muons. Peak values of the muon asymmetry are close to those obtained for the D -meson and lie in the range 0.75% to 11%.

PACS numbers: 13.88.+e, 13.60.-r, 14.40.Lb, 29.25.Pj

* rohini@chepr.iisc.ernet.in

† abhiramb@chepr.iisc.ernet.in

‡ misra@physics.mu.ac.in

I. INTRODUCTION

Transverse single-spin asymmetries (SSA) can be a vital source of information on the three-dimensional structure of hadrons and have hence been the subject of increasing interest in the past two decades. While they have been observed since the mid-70s in the hadroproduction of pions, i.e., $p^\uparrow p \rightarrow \pi + X$ [1–3], the past few years have provided a large amount of high quality data on SSAs in a wide variety of processes such as $p^\uparrow p \rightarrow \pi + X$, $p^\uparrow p \rightarrow K^\pm + X$, $p^\uparrow p \rightarrow J/\psi + X$, $lp^\uparrow \rightarrow \pi + X$, $lp^\uparrow \rightarrow K + X$ etc., (see Refs. [4, 5] for reviews on the subject). A theoretical approach based on factorisation in terms of a hard-part and transverse momentum dependent (TMD) parton distribution functions (PDFs) and fragmentation function (FFs) has been formally established for two-scale processes, which have a hard energy scale, such as the virtuality of the photon in the Drell-Yan process and a relatively soft scale of the order of Λ_{QCD} , such as the transverse momentum of the Drell-Yan lepton-pair. Another approach based on factorisation in terms of twist-3 parton correlators has been shown to be valid for the description of SSAs in processes with a single hard scale such as the transverse momentum of a pion in hadronic collisions.

Despite the absence of a formal proof, a lot of work has been done on a TMD description of single hard-scale processes under the assumption of factorisation, in what is generally referred to as the generalised parton model (GPM) approach. This approach has been quite successful in describing unpolarised cross-sections in the hadroproduction of pions [6]. The leading-order (LO) GPM is able to better describe (upto a K-factor) experimental data on pion production in high energy hadron-hadron collisions than either LO or NLO collinear pQCD. It is also able to provide a good description of data on SSA in $p^\uparrow p \rightarrow \pi + X$ at widely different c.o.m energies [4]. One of the important transverse-momentum-dependent distributions which can lead to SSAs is the Sivers distribution [7, 8], which encodes the correlation between the azimuthal anisotropy in the distribution of an unpolarised parton and the spin of its parent hadron. This anisotropy in the parton’s transverse momentum distribution can lead to an azimuthal anisotropy in the distribution of the inclusive final state, i.e., an SSA. Fits of the u and d quark Sivers functions (QSF) on data on $A_N(p^\uparrow p \rightarrow \pi + X)$ at E704 ($\sqrt{s} = 19.4$ GeV) do a good job of describing the main features of the asymmetry observed at STAR ($\sqrt{s} = 200$ GeV) [4]. While the quark Sivers functions have been widely studied over the years, the gluon Sivers function (GSF) remains poorly understood.

A first indirect estimate of the gluon Sivers function in a GPM framework was performed in Ref. [9]. The analysis consisted of fitting the GSF to midrapidity data on SSA in pion production at RHIC. In it, the quark contribution to the SSA was calculated by using quark Sivers functions (QSF) as extracted from semi-inclusive deep inelastic scattering data. The GSF fits obtained by the analysis give asymmetries much smaller than allowed by the positivity bound. On the other hand, a recent study of large- p_T hadron pair production in COMPASS indicates a substantial negative gluon Sivers asymmetry for both proton and deuteron targets [10]. It is true that this is a more direct probe of the gluon as large- p_T hadron pairs are produced through the photon-gluon fusion process, however the final state also receives contributions from the QCD Compton process, which is quark initiated. Hence an extraction of the GSF using large- p_T hadron production is contaminated by the quark contributions to the SSA and would therefore depend on the extent to which these different processes can be separated in a data sample. With this being the first significant evidence for a non-zero GSF, it is important to study processes such as closed and open charm production which probe the gluon channel cleanly and directly.

In this work, using a GPM approach, we study the low-virtuality lepton production ($Q^2 \approx 0$) of open-charm as a possible probe of the poorly understood gluon Sivers function (GSF). At the leading-order (LO) of this process, the production of open-charm happens only via photon-gluon fusion (PGF), making it a direct probe of the gluon content of the proton. The GPM study of open-charm production as a probe of the gluon Sivers function was first proposed in Ref. [11] for the process $p^\uparrow p \rightarrow D^0 + X$. In that study they considered two extreme scenarios for the GSF: zero and maximal. The term ‘maximal’ here refers to the Sivers function with its positivity bound of twice the unpolarised TMD ($|\Delta^N f_{i/p^\uparrow}(x, \mathbf{k}_\perp)|/2f_{i/p}(x, \mathbf{k}_\perp) \leq 1$), saturated for all values of x — we shall refer to this as the ‘saturated’ Sivers function henceforth. Their study indicated that a measurement of SSA at RHIC for this process can give a direct indication of a nonzero gluon Sivers function.

The low-virtuality lepton production of J/ψ has also been suggested as a probe of the GSF [12–14]. However, lepton production of open-charm may have some more advantages over the above mentioned processes. Firstly, unlike the case with $p^\uparrow p \rightarrow D^0 + X$, one need not worry about possible factorisation breaking initial state interactions. $p^\uparrow l \rightarrow D^0 + X$ would have the same initial/final state interactions as SIDIS, for which TMD factorisation has been established. A study of SSA in this process might therefore complement studies

of SSA in SIDIS and $lp^\uparrow \rightarrow h + X$ [15, 16] by providing an additional handle on the gluon Sivers function. Secondly, open-charm production is not affected by issues of production model dependence as is the case with closed-charm [17].

We therefore consider the process $lp^\uparrow \rightarrow D^0 + X$ in the low-virtuality regime in a GPM framework and see how it could serve as a probe of the GSF at both COMPASS and a future Electron-Ion Collider (EIC). While present data on open-charm production in COMPASS may be limited due to statistics, the proposed Electron-Ion Collider [18] would have a significantly higher luminosity and should be able to provide better data on open/closed charm production. For both experiments, we present estimates for the maximum magnitude of SSA as obtained using the saturated GSF, and also the expected values of SSA obtained using the fits of Ref. [9].

In section II, we give the expressions for the relevant quantities in the GPM framework. In section III, we give the parametrisations for the different TMDs used, and in section IV, we discuss the results for both COMPASS and EIC kinematics.

II. THE GPM FORMALISM

In this work, we are concerned with the single-spin asymmetry in the low-virtuality lepton production of open charm,

$$A_N = \frac{d\sigma^\uparrow - d\sigma^\downarrow}{d\sigma^\uparrow + d\sigma^\downarrow} \quad (1)$$

where $d\sigma^{\uparrow(\downarrow)}$ is the invariant differential cross-section for the process $p^{\uparrow(\downarrow)}l \rightarrow D + X$ with the spin of the transversely polarised proton being aligned in the $\uparrow(\downarrow)$ direction with respect to the production plane. Here, \uparrow would be the $+Y$ direction in a frame where the polarised proton is moving along the $+Z$ direction and the meson is produced in the XZ plane.

Following the treatment of open-charm hadroproduction [11], we can write the denominator and numerator of Eq. 1 as,

$$\begin{aligned} d\sigma^\uparrow + d\sigma^\downarrow &= \frac{E_D d\sigma^{p^\uparrow l \rightarrow DX}}{d^3 \mathbf{p}_D} + \frac{E_D d\sigma^{p^\downarrow l \rightarrow DX}}{d^3 \mathbf{p}_D} = 2 \frac{E_D d\sigma^{pl \rightarrow DX}}{d^3 \mathbf{p}_D} \\ &= \int dx_g dx_\gamma dz d^2 \mathbf{k}_{\perp g} d^2 \mathbf{k}_{\perp \gamma} d^3 \mathbf{k}_D \delta(\mathbf{k}_D \cdot \hat{\mathbf{p}}_c) \delta(\hat{s} + \hat{t} + \hat{u} - 2m_c^2) \mathcal{C}(x_g, x_\gamma, z, \mathbf{k}_D) \\ &\quad \times f_{g/p}(x_a, \mathbf{k}_{\perp g}) f_{\gamma/l}(x_\gamma, \mathbf{k}_{\perp \gamma}) \frac{d\hat{\sigma}^{g\gamma \rightarrow c\bar{c}}}{d\hat{t}}(x_g, x_\gamma, \mathbf{k}_{\perp g}, \mathbf{k}_{\perp \gamma}, \mathbf{k}_D) D_{D/c}(z, \mathbf{k}_D) \end{aligned} \quad (2)$$

and

$$\begin{aligned}
d\sigma^\uparrow - d\sigma^\downarrow &= \frac{E_D d\sigma^{p^\uparrow l \rightarrow DX}}{d^3 \mathbf{p}_D} - \frac{E_D d\sigma^{p^\downarrow l \rightarrow DX}}{d^3 \mathbf{p}_D} \\
&= \int dx_g dx_\gamma dz d^2 \mathbf{k}_{\perp g} d^2 \mathbf{k}_{\perp \gamma} d^3 \mathbf{k}_D \delta(\mathbf{k}_D \cdot \hat{\mathbf{p}}_c) \delta(\hat{s} + \hat{t} + \hat{u} - 2m_c^2) \mathcal{C}(x_g, x_\gamma, z, \mathbf{k}_D) \\
&\quad \times \Delta^N f_{g/p^\uparrow}(x_a, \mathbf{k}_{\perp g}) f_{\gamma/l}(x_\gamma, \mathbf{k}_{\perp \gamma}) \frac{d\hat{\sigma}^{g\gamma \rightarrow c\bar{c}}}{d\hat{t}}(x_g, x_\gamma, \mathbf{k}_{\perp g}, \mathbf{k}_{\perp \gamma}, \mathbf{k}_D) D_{D/c}(z, \mathbf{k}_D).
\end{aligned} \tag{3}$$

In the above expressions, $x_{g(\gamma)}$ is the light-cone momentum fraction of the incoming gluon (photon) along the parent proton (lepton) direction, $z = p_D^+/p_c^+$ is the light-cone momentum fraction of the D -meson along the fragmenting charm quark direction, $\mathbf{k}_{g(\gamma)}$ is the intrinsic transverse momentum of the gluon (photon) with respect to the parent particle direction, \mathbf{k}_D is the transverse momentum with which the meson fragments from the charm quark, $\hat{\mathbf{p}}$ is the unit vector along the heavy quark direction, m_c is the charm quark mass, and \hat{s} , \hat{t} and \hat{u} are the Mandelstam variables for the photon-gluon fusion process $\gamma g \rightarrow c\bar{c}$.

The expressions $\Delta^N f_{g/p^\uparrow}(x, \mathbf{k}_\perp)$ and $f_{g/p}(x, \mathbf{k}_\perp)$ are the gluon Sivers function and unpolarised TMD respectively. $f_{\gamma/l}(x, \mathbf{k}_\perp)$ is the transverse-momentum-dependent distribution of quasi-real photons in an unpolarised lepton, and $D_{D/c}(z, \mathbf{k}_D)$ is the transverse-momentum-dependent fragmentation function. The functional forms of all of these distributions are given in Sec. III.

The Sivers function, $\Delta^N f_{i/p^\uparrow}(x, k_\perp; Q)$ describes the azimuthal anisotropy in the transverse momentum distribution of unpolarised partons inside a transversely polarised proton,

$$\begin{aligned}
f_{i/p^\uparrow}(x, \mathbf{k}_\perp, \mathbf{S}; Q) &= f_{i/p}(x, k_\perp; Q) + \frac{1}{2} \Delta^N f_{i/p^\uparrow}(x, k_\perp; Q) \frac{\epsilon_{ab} k_\perp^a S^b}{k_\perp} \\
&= f_{i/p}(x, k_\perp; Q) + \frac{1}{2} \Delta^N f_{i/p^\uparrow}(x, k_\perp; Q) \cos \phi_\perp
\end{aligned} \tag{4}$$

where $\mathbf{k}_\perp = k_\perp(\cos \phi_\perp, \sin \phi_\perp)$. In a generalised parton model (GPM) description of this process, the only possible source of an asymmetry would be a non-zero gluon Sivers function. There cannot be any contribution from the Collins effect since photon-gluon fusion results in unpolarized final state quarks.

The partonic cross-section for photon-gluon fusion into a heavy quark pair is given by [19],

$$\begin{aligned}
\frac{d\hat{\sigma}^{g\gamma \rightarrow c\bar{c}}}{d\hat{t}} &= \frac{4\pi}{8 \times 9} \frac{\alpha_{\text{em}} \alpha_s}{\hat{s}^2 (\hat{t} - m_c^2)^2 (\hat{u} - m_c^2)^2} [-(\hat{t} - \hat{u})^4 - 4\hat{s}(\hat{t} + \hat{u})(\hat{t} - \hat{u})^2 \\
&\quad - 4\hat{s}^2 ((\hat{t} - \hat{u})^2 + 2(\hat{t} + \hat{u})^2) - 12\hat{s}^3(\hat{t} + \hat{u}) - 3\hat{s}^4]
\end{aligned} \tag{5}$$

where the Mandelstam variables are defined in the usual way,

$$\hat{s} = (P_g + P_\gamma)^2; \hat{t} = (P_g - P_c)^2; \hat{u} = (P_\gamma - P_c)^2, \quad (6)$$

and the factor $\mathcal{C}(x_g, x_\gamma, z, \mathbf{k}_D)$ contains the parton flux and the Jacobian relating the partonic phase-space and the mesonic phase-space,

$$\mathcal{C}(x_g, x_\gamma, z, \mathbf{k}_D) = \frac{\hat{s}}{\pi z^2} \frac{\hat{s}}{x_g x_\gamma s} \frac{\left(E_D + \sqrt{\mathbf{p}_D^2 - \mathbf{k}_{\perp D}^2}\right)^2}{4(\mathbf{p}_D^2 - \mathbf{k}_{\perp D}^2)} \left[1 - \frac{z^2 m_c^2}{\left(E_D + \sqrt{\mathbf{p}_D^2 - \mathbf{k}_{\perp D}^2}\right)^2}\right]^2 \quad (7)$$

The on-shell condition $\hat{s} + \hat{t} + \hat{u} = 2m_c^2$, gives a quartic equation in z and hence z can be fixed by using it as shown in Ref. [20].

The delta function $\delta(\mathbf{k}_D \cdot \hat{\mathbf{p}}_c)$ ensures that the region of integration for \mathbf{k}_D is confined to the two-dimensional plane perpendicular to the direction of the charm quark i.e.,

$$\int d^3 \mathbf{k}_D \delta(\mathbf{k}_D \cdot \hat{\mathbf{p}}_c) D_{D/c}(z, \mathbf{k}_D) \dots = \int d^2 \mathbf{k}_{\perp D} D_{D/c}(z, \mathbf{k}_{\perp D}) \dots \quad (8)$$

where $\mathbf{k}_{\perp D}$ represents values of transverse momenta on the allowed plane.

An outline of the treatment of the parton level kinematics and the TMD fragmentation are given in the appendix.

III. PARAMETRISATION OF THE TMDS

Since we give predictions using the GSF fits of Ref. [9], for consistency we have to use the unpolarised gluon TMD and Sivers function used therein. We use standard factorised Gaussian form for the unpolarised gluon TMD,

$$f_{g/p}(x, k_\perp; Q) = f_{g/p}(x, Q) \frac{1}{\pi \langle k_\perp^2 \rangle} e^{-k_\perp^2 / \langle k_\perp^2 \rangle} \quad (9)$$

with $\langle k_\perp^2 \rangle = 0.25 \text{ GeV}^2$. We model the photon distribution $f_{\gamma/l}(x, \mathbf{k}_\perp)$ in a similar way by assuming a Gaussian transverse momentum dependence for the photons [12–14],

$$f_{\gamma/l}(x_\gamma, \mathbf{k}_{\perp\gamma}; s) = f_{\gamma/l}(x, s) \frac{1}{\pi \langle k_{\perp\gamma}^2 \rangle} e^{-k_{\perp\gamma}^2 / \langle k_{\perp\gamma}^2 \rangle} \quad (10)$$

with $\langle k_{\perp\gamma}^2 \rangle = 0.1 \text{ GeV}^2$. Here $f_{\gamma/l}(x_\gamma, s)$ is the standard Weizsäcker-Williams distribution of quasi-real photons [21–23]. A first attempt towards a TMD distribution of photons in

a lepton, calculated from first principles, has been made in Ref. [24]. However, we do not consider it in this work.

As with the unpolarised densities, we take the transverse-momentum-dependence of the FF to be Gaussian,

$$D_{D/c}(z, \mathbf{k}_D) = D_{D/c}(z) \frac{1}{\pi \langle k_{\perp D}^2 \rangle} e^{-k_D^2 / \langle k_{\perp D}^2 \rangle} \quad (11)$$

with $\langle k_{\perp D}^2 \rangle = 0.25 \text{ GeV}^2$.

The gluon Sivers function is parametrised in the standard way as follows,

$$\Delta^N f_{g/p^\uparrow}(x, \mathbf{k}_\perp; Q) = 2\mathcal{N}_g(x) f_{g/p}(x, Q) \frac{\sqrt{2e}}{\pi} \sqrt{\frac{1-\rho}{\rho}} k_\perp \frac{e^{-k_\perp^2 / \rho \langle k_\perp^2 \rangle}}{\langle k_\perp^2 \rangle^{3/2}} \quad (12)$$

with $0 < \rho < 1$. $\mathcal{N}_g(x)$ parametrises the x -dependence of the GSF and is generally written as

$$\mathcal{N}_g(x) = N_g x^{\alpha_g} (1-x)^{\beta_g} \frac{(\alpha_g + \beta_g)^{\alpha_g + \beta_g}}{\alpha_g^{\alpha_g} \beta_g^{\beta_g}} \quad (13)$$

It must obey $|\mathcal{N}_g(x)| < 1$ in order for the Sivers function to satisfy the positivity bound,

$$\frac{|\Delta^N f_{g/p^\uparrow}(x, \mathbf{k}_\perp)|}{2f_{g/p}(x, \mathbf{k}_\perp)} \leq 1 \quad \forall x, \mathbf{k}_\perp. \quad (14)$$

In this work, for the predictions with DGLAP evolved densities we consider,

1. the Sivers function with the positivity bound saturated, i.e., $\mathcal{N}_g(x) = 1$ and $\rho = 2/3$.
2. the SIDIS1 and SIDIS2 extractions of the Sivers function from Ref. [9].

As mentioned in the introduction, we will refer to the first choice as the ‘saturated’ Sivers function. It would give an upper bound on the asymmetry for a fixed width $\langle k_\perp^2 \rangle$. The parameter ρ is set to 2/3 in order to maximize the contribution from the transverse dependent part [25]. It must be kept in mind though, that it cannot be treated as giving an absolute upper bound on A_N — an increased width, $\langle k_\perp^2 \rangle$ naturally results in increased asymmetry since the effects of the parton transverse momenta are more pronounced.

The SIDIS1 and SIDIS2 GSFs from Ref. [9] are the first (and so far, only) available extractions of the GSF in a GPM framework. They were obtained by fitting to PHENIX data on A_N in inclusive pion production in the midrapidity region at RHIC. The two differ in the choice of quark Sivers functions and associated light quark fragmentation functions that were used in the fit. The QSF set used in obtaining SIDIS1 [26] contained only u and d flavours, and was fitted to data on pion production in HERMES and positive hadron

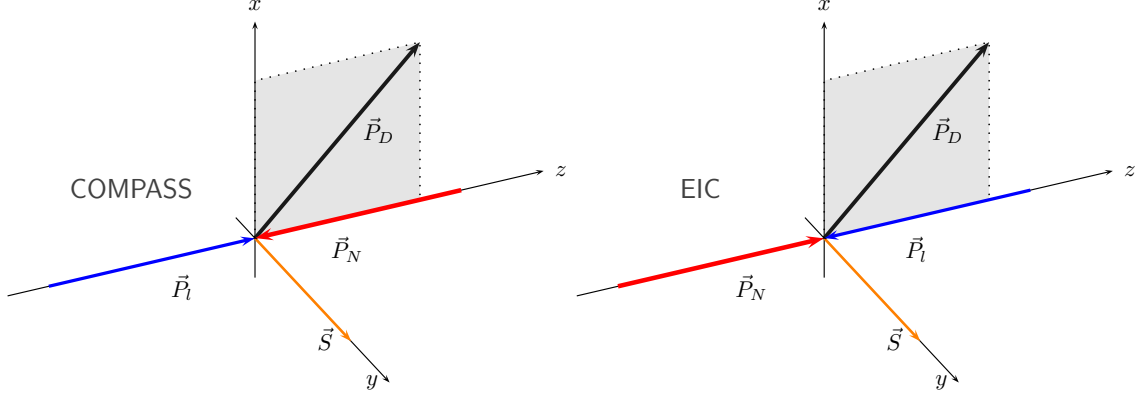


FIG. 1. Kinematics for COMPASS (left) and EIC (right). \vec{P}_N is the proton momentum and \vec{S} is its spin orientation. \vec{P}_l is the lepton momentum. The D -meson momentum, \vec{P}_D is taken to be on the x - z plane.

production in COMPASS with fragmentation functions by Kretzer [27]. The QSF set used for SIDIS2 [28] was fitted to flavour segregated data on pion and kaon production and hence included sea quark Sivers functions as well. It used fragmentations by de Florian, Sassot and Stratmann (DSS) [29]. The two fits show very different x -dependencies, with SIDIS1 being larger in the moderate- x region and SIDIS2 being larger in the low- x region. The values of the parameters of the two GSF fits are given in Table I.

SIDIS1	$N_g = 0.65$	$\alpha_g = 2.8$	$\beta_g = 2.8$	$\rho = 0.687$	$\langle k_\perp^2 \rangle = 0.25 \text{ GeV}^2$
SIDIS2	$N_g = 0.05$	$\alpha_g = 0.8$	$\beta_g = 1.4$	$\rho = 0.576$	

TABLE I. Parameters of the GSF fits from Ref. [9].

IV. NUMERICAL ESTIMATES

In this section we present results on the unpolarised cross-section and SSA for COMPASS and EIC kinematics. Before going into the results, we should first make a note on the differing kinematic conventions of the two experiments: As COMPASS is a fixed target experiment, by convention the lepton is taken to be along the $+z$ direction. This means that, in the definition of A_N in Eq. 1, keeping the conventions for proton spin direction and production plane the same, positive x_F and η correspond to the backward hemisphere of the proton, whereas negative x_F and η correspond to the forward hemisphere of the proton. Note that

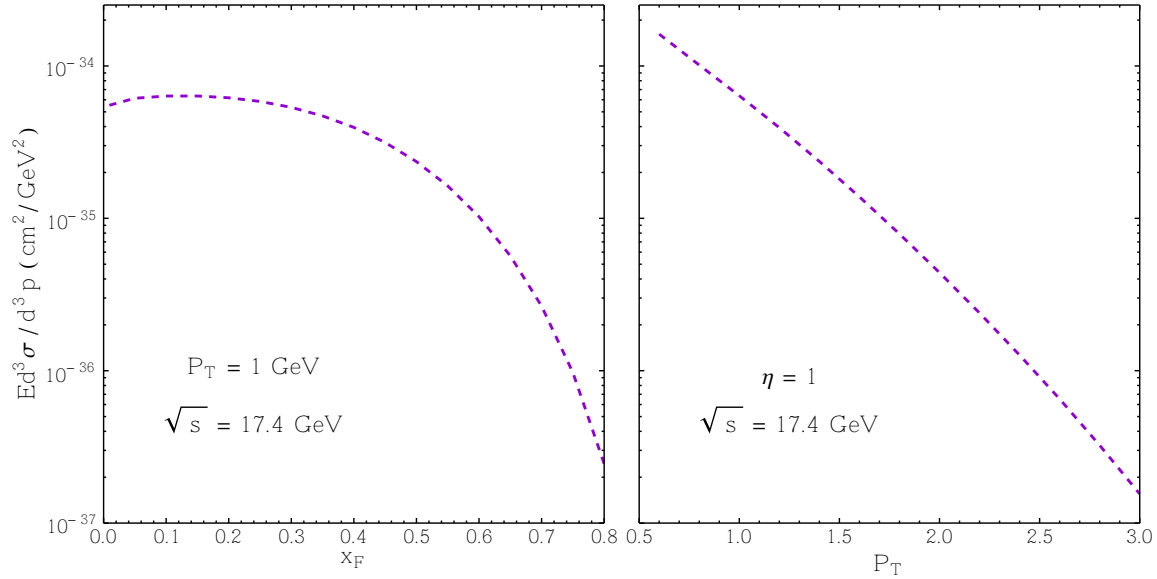


FIG. 2. Unpolarized cross-section at COMPASS as a function of x_F (at fixed P_T , left panel) and P_T (at fixed η , right panel).

this convention differs from that adopted Sec. II where, following the RHIC convention, the *proton* is taken to be moving along the $+z$ direction. Since EIC, like RHIC, is also a collider experiment, we shall use the same convention for it. In the interest of clarity, the conventions used for the two experiments are illustrated in Fig. 1.

The numerical results were obtained using the GRV98LO set for the collinear gluon density and for the collinear part of the FF, the LO parameterisation by Kniehl and Kramer [30] was used. The QCD scale was chosen to be $Q^2 = m_D^2 + P_T^2$.

A. COMPASS

The COMPASS experiment is a fixed target experiment involving a 160 GeV muon beam colliding on a proton target with a resulting centre of mass energy $\sqrt{s} = 17.4$ GeV. The COMPASS spectrometer covers hadrons in the l - p c.o.m pseudorapidity range $-0.1 < \eta_h < 2.4$ and can detect D^0 mesons through their $D^0 \rightarrow K^-\pi^+$ decay mode. The geometry of the detector allows the proper reconstruction of the D^0 's produced only in the backward hemisphere of the proton and hence we restrict our analysis to the $x_F, \eta > 0$ region.

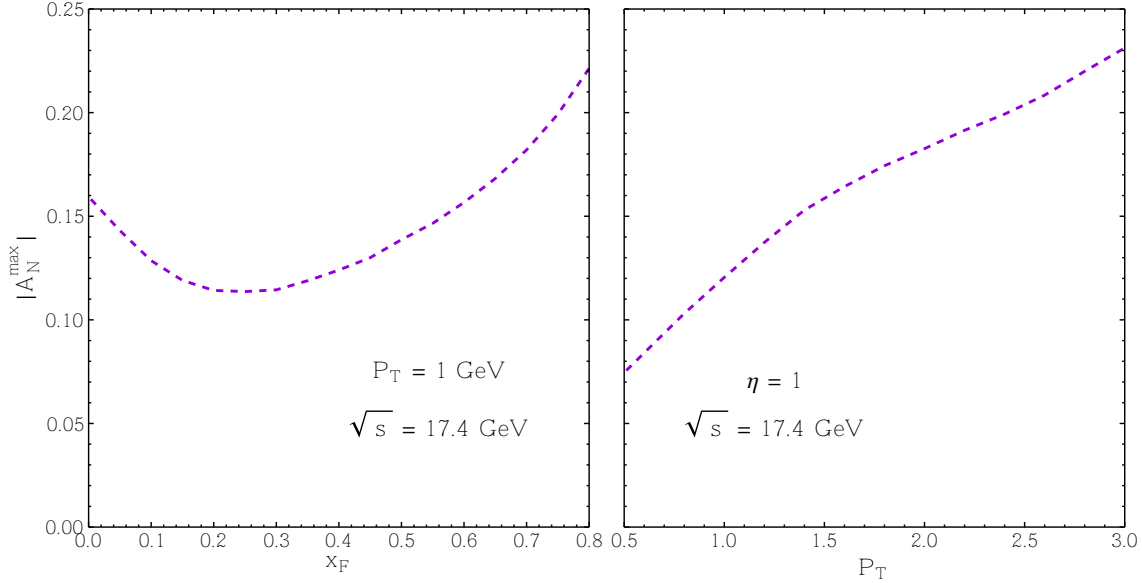


FIG. 3. SSA with saturated GSF at COMPASS as a function of x_F (at fixed P_T , left panel) and P_T (at fixed η , right panel).

In Fig. 2, we show results for the unpolarised invariant cross-section as a function of x_F at fixed $P_T = 1 \text{ GeV}$ (left panel) and as a function of P_T at a fixed pseudorapidity $\eta = 1$ (right panel). At a fixed P_T , the cross-section varies by two orders of magnitude in the region $0 < x_F < 0.8$. At fixed pseudorapidity, the cross-section decreases with increasing P_T by three orders of magnitude in the range $0.5 < P_T < 3.0$. For a larger choice of the unpolarised TMD width, $\langle k_\perp^2 \rangle = 1 \text{ GeV}^2$, the cross-section at fixed P_T is not affected much whereas, the cross-section at fixed pseudorapidity slightly spreads out in P_T — becoming slightly smaller for lower P_T values and slightly larger for higher P_T values — as one would expect. Overall, cross-section estimates for COMPASS are not very sensitive to the unpolarised TMD width. Changes in the width of the TMD FF in the range $0 < \langle k_{\perp D}^2 \rangle < 0.25 \text{ GeV}^2$ also do not affect the cross-section significantly.

Fig. 3 shows estimates for the maximum value of the magnitude of the asymmetry $|A_N^{\max}|$, obtained by using the saturated gluon Sivers function viz., $\mathcal{N}_g(x) = 1$, $\rho = 2/3$. The results are presented as a function of x_F at fixed $P_T = 1 \text{ GeV}$ (left panel) and as a function of P_T at a fixed pseudorapidity $\eta = 1$ (right panel). At fixed $P_T = 1 \text{ GeV}$, estimates of $|A_N^{\max}|$ range from a minimum of 11% at $x_F = 0.2$ to upto 22% at $x_F = 0.8$. At fixed $\eta = 1$, $|A_N^{\max}|$

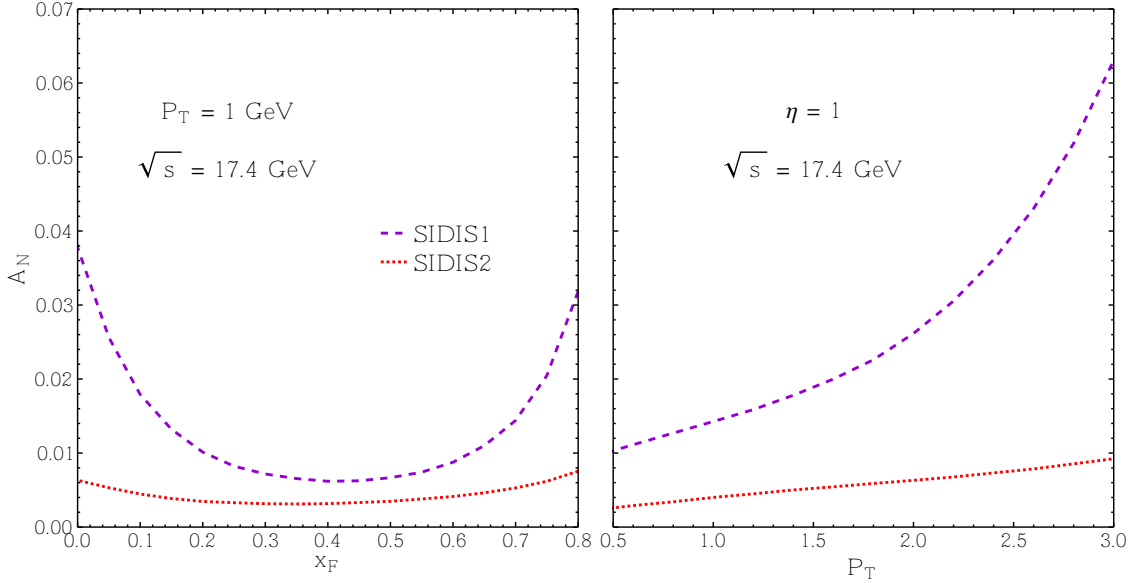


FIG. 4. SSA from GSF fits of Ref. [9] at COMPASS as a function of x_F (at fixed P_T , left panel) and P_T (at fixed η , right panel).

shows a general increase with the meson transverse momentum, ranging from around 7% at $P_T = 0.5$ GeV to 18% at $P_T = 3$ GeV.

Fig. 4 shows the asymmetries obtained using the SIDIS1 and SIDIS2 fits [9]. In general, while both fits give asymmetries much smaller than allowed by the positivity bound, SIDIS2 give asymmetries much smaller than those obtained with SIDIS1. This is because the kinematic regions we consider sample the region $0.08 < x_a < 0.5$, where SIDIS1 is much larger than SIDIS2, as can be seen from the numbers in Table I. At fixed P_T , SIDIS1 gives a peak asymmetry of 3.8% at $x_F = 0$ and SIDIS2 gives a peak asymmetry of 0.8% at $x_F = 0.8$. At fixed $\eta = 1$, SIDIS1 gives a peak asymmetry of 6.3% and SIDIS1 gives a peak asymmetry of almost 1%, both at $P_T = 3.0$ GeV. We have verified that changes in the width of the TMD FF in the range $0 < \langle k_{\perp D}^2 \rangle < 0.25$ GeV 2 do not alter the results for either SIDIS1 or SIDIS2 substantially and the general features of the A_N predictions stay the same. Though it is not a straightforward comparison, note that the predictions of small A_N obtained using these fits, stand in contrast to the relatively large gluon contribution to the asymmetry that was found in large- p_T hadron pair production [10].

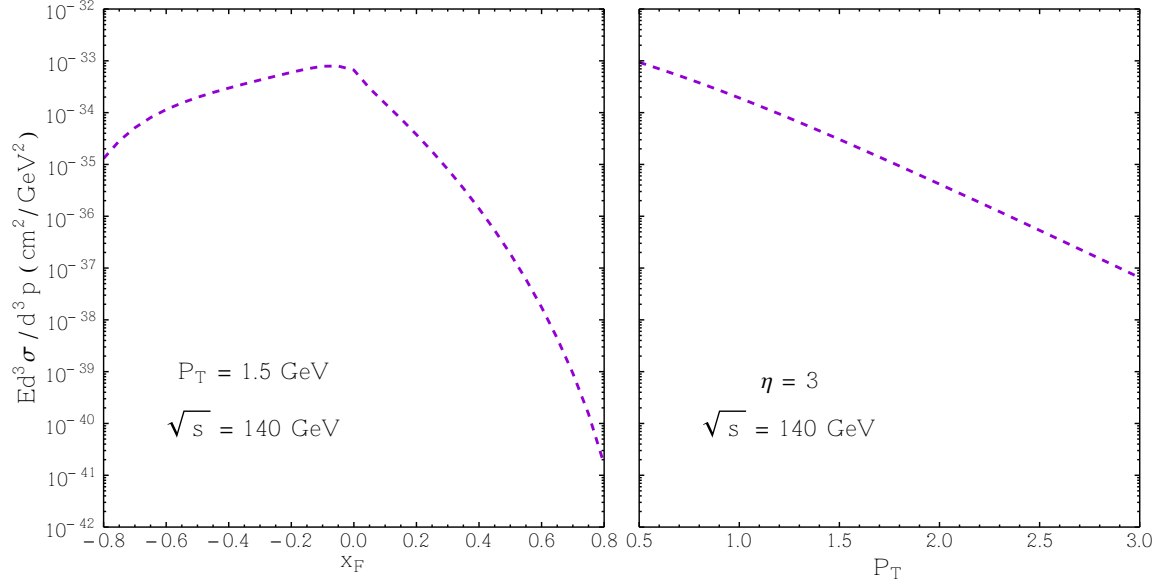


FIG. 5. Unpolarized cross-section at EIC as a function of x_F (at fixed P_T , left panel) and P_T (at fixed η , right panel).

B. EIC

The Electron-Ion Collider (EIC) is a proposed experiment electron and proton/ion beams, with the possibility of both being polarised. It is meant to be capable of attaining high luminosities with a centre of mass energy of upto 140 GeV in the ep configuration.

In Fig. 5, we show results for the unpolarised invariant cross-section as a function of x_F at fixed $P_T = 1.5$ GeV (left panel) and as a function of P_T at a fixed pseudorapidity $\eta = 3$ (right panel). At fixed P_T , in the forward region, the cross-section decreases with increasing x_F by more than six orders of magnitude in the range $0 < x_F < 0.7$. In contrast, in the backward region, decrease in the cross-section with increasing $|x_F|$ is only around an order of magnitude. This is due to the $1/x_\gamma$ enhancement in the Weiszacker-Williams distribution at low x_γ . At fixed η , the cross-section decreases with increasing P_T by four orders of magnitude in the range $0.5 < P_T < 3.0$ GeV. With a larger choice of the unpolarised TMD width $\langle k_\perp^2 \rangle = 1.0$ GeV 2 , the cross-section at fixed P_T is found to be unaffected in the forward region, but shows a decrease in the backward region of about 40% on average. The increase in the P_T -spread of the cross-section is also observed at fixed η , but the effect is very small.

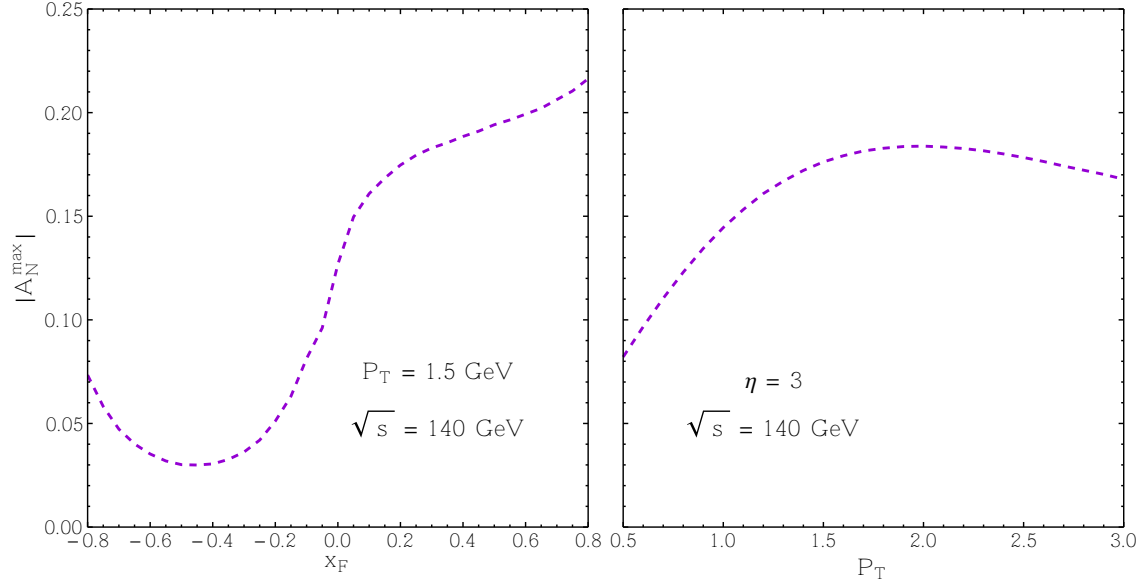


FIG. 6. SSA with saturated GSF at EIC as a function of x_F (at fixed P_T , left panel) and P_T (at fixed η , right panel).

The cross-section is also found to be insensitive to changes in the width of the fragmentation function in the range $0 < \langle k_{\perp D}^2 \rangle < 0.25 \text{ GeV}^2$.

In Fig. 6, we show estimates for the maximum value of the magnitude of the asymmetry $|A_N|$, obtained by using the saturated gluon Sivers function, as a function of x_F at fixed $P_T = 1.5 \text{ GeV}$ (left panel) and as a function of P_T at fixed pseudorapidity $\eta = 3$ (right panel). With EIC having a fairly large centre of mass energy, we find that the general features of $|A_N^{\max}|$ are similar to what was obtained for proton-proton collisions at RHIC [11, 20]. At fixed $\eta = 3$, the asymmetry peaks at almost 19% at $P_T = 2 \text{ GeV}$. At fixed P_T , large asymmetries are allowed in the forward region, with estimates being greater than 20% for $x_F > 0.5$. As is the case at RHIC, the asymmetry is suppressed in the backward hemisphere of the proton ($x_F < 0$). This is because, in the backward region, the hard-part $d\sigma/d\hat{t}$ depends very weakly on the azimuthal angle of the gluon transverse momentum $\phi_{\perp g}$. This weak dependence, along with the $\cos \phi_{\perp g}$ term that is present in the Sivers function (see Eq. 4) leads to a suppression when the azimuthal angle is integrated over. The same has been observed in Ref. [11]. It must be mentioned however, that this suppression is weaker at lower centre of mass energies, as can be seen from the large values of $|A_N^{\max}|$ at $x_F \gtrsim 0.3$.

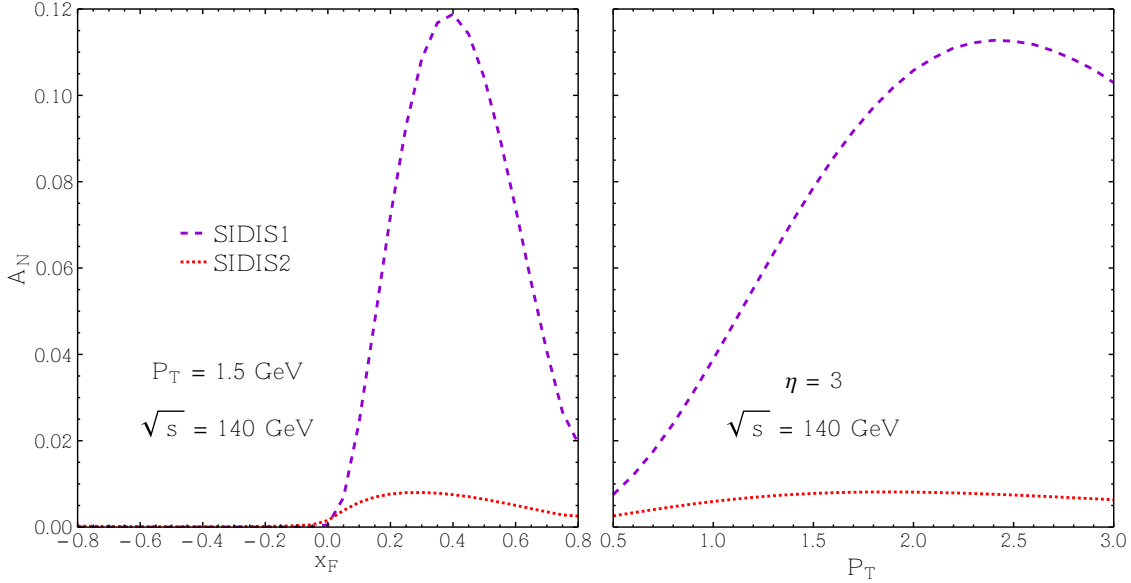


FIG. 7. SSA from GSF fits of Ref. [9] at EIC as a function of x_F (at fixed P_T , left panel) and P_T (at fixed η , right panel).

for COMPASS shown in Fig. 3.

Fig. 7 shows the asymmetries obtained using the SIDIS1 and SIDIS2 fits [9]. As was the case for COMPASS kinematics, both fits give asymmetries much smaller than allowed by the positivity bound. At fixed P_T , in the forward region, SIDIS1 gives significantly larger asymmetries than SIDIS2. SIDIS1 gives a peak asymmetry of almost 12% at $x_F = 0.4$ and SIDIS2 gives a peak asymmetry of 0.8% at $x_F = 0.3$. In the backward region $x_F < 0$, D production gets contributions mainly from $x_a < 0.08$, where SIDIS2 is larger than SIDIS1. However the overall values of both fits in this region are very small. Combined with the azimuthal suppression, this makes the asymmetries from both fits almost negligible. At fixed pseudorapidity, SIDIS1 gives a peak asymmetry of around 11% at $P_T = 2.5$ GeV and SIDIS2 gives a peak asymmetry of around 0.8% at $P_T = 1.6-2.2$ GeV.

So far we have considered the SSA in terms of the D -meson kinematics. It would also be interesting to consider the SSA in terms of the kinematics of the decay muons. A detector such as the proposed ePHENIX [31] would be able to study open heavy flavour production through the leptonic decay channels. With this in mind, we consider the semileptonic decay of the D 's in order to obtain the SSA for the decay muons, A_N^μ . The results for the

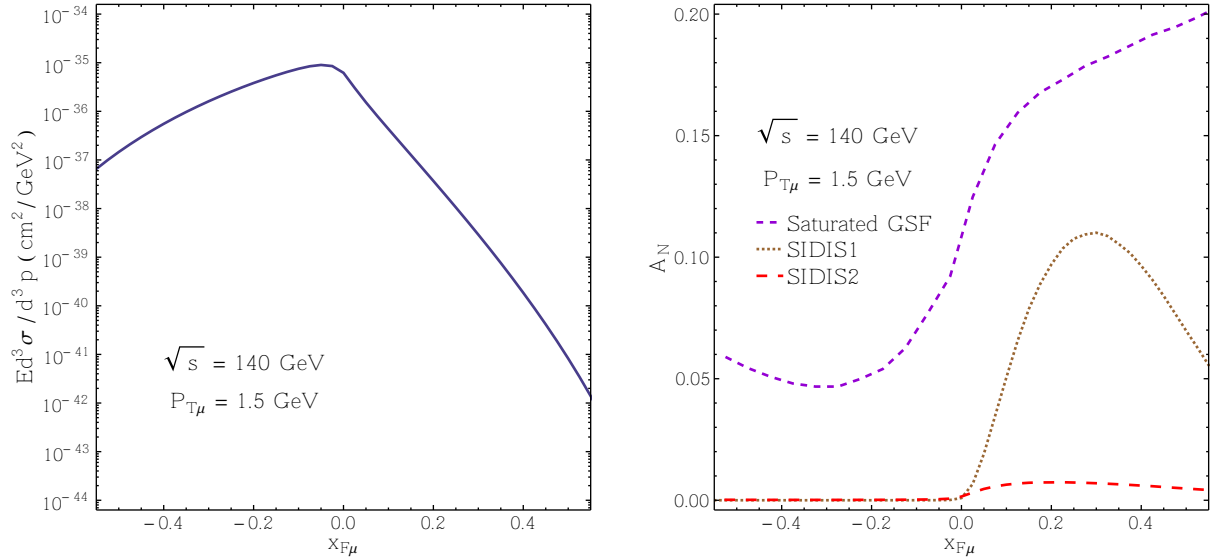


FIG. 8. Cross-section (left panel) and SSA (right panel) for decay-muons.

SSA with a saturated GSF for the decay muons are presented in Fig. 8 as a function of $x_{F\mu} = 2P_{L\mu}/\sqrt{s}$, with the muon transverse momentum $P_{T\mu} = 1.5 \text{ GeV}$. It appears that an azimuthal anisotropy in D production would be retained significantly in the decay-muons. The general dependence of the muon SSA on $x_{F\mu}$ is similar to the dependence of the D -meson SSA on x_F . As with the D -meson, the muon SSA is also suppressed in the backward hemisphere. Peak values of the muon A_N^μ are close to those obtained for the meson: With the SIDIS1 GSF, A_N^μ has a peak value of 11% at $x_{F\mu} = 0.3$ whereas A_N has a peak value of almost 12% at $x_F = 0.4$. With the SIDIS2 GSF, A_N^μ has a peak value of 0.75% at $x_{F\mu} = 0.23$ whereas A_N has a peak value of 0.8% at $x_F = 0.3$.

V. CONCLUSIONS

In this work, we have presented results for SSA in the low-virtuality lepto-production of open-charm at both COMPASS and a future Electron-Ion Collider. We find that an asymmetry of upto around 20% is allowed by the saturated gluon Sivers function at both COMPASS and EIC. We also find that, for EIC kinematics, the asymmetry is significantly retained in the distribution of the decay muons.

This two GSF fits of Ref. [9] for which we give predictions, were extracted from data on midrapidity pion production at RHIC. As mentioned earlier, the two differ in the choices of QSF parameters and light quark fragmentation functions used in the extraction. Though they both describe their input data equally well, they show widely differing x -dependencies.

In this work, we find that the lepton production of open-charm, which probes the gluon content of the proton directly, is able to discriminate well between these two fits. Thus we see that this process offers a good probe of the gluon Sivers function. In general, at COMPASS and in the forward region of EIC, SIDIS2 gives small, but non-negligible asymmetry predictions on the level of significant fractions of a percent, whereas SIDIS1 predicts larger asymmetries of the order of a few percent. This indicates that the lepton production of open-charm could be a vital probe in constraining the gluon Sivers function, and also in testing the validity of the GPM framework.

VI. ACKNOWLEDGEMENTS

R.M.G. wishes to acknowledge support from the Department of Science and Technology, India under Grant No. SR/S2/JCB-64/2007 under the J.C. Bose Fellowship scheme. A.M would like to thank the Department of Science and Technology, India for financial support under Grant No.EMR/2014/0000486. A.M would also like to thank the Theory Division, CERN, Switzerland for their kind hospitality.

VII. APPENDIX

In this work, we have considered inclusive single-particle lepton production in the low virtuality regime. This allows us to handle the process in terms of a TMD distribution of quasi-real photons in a lepton, not unlike a TMD distribution of partons in a hadron. The treatment of parton kinematics here is thus similar to the treatment of transverse-momentum-dependent parton kinematics for inclusive single-particle hadroproduction, which can be found in quite a few places [32, 33] including Ref. [6], where heavy meson final states have been considered.

The momenta of the proton, lepton and the D -meson can be written in the $p-l$ centre of mass frame as,

$$P_P = \frac{\sqrt{s}}{2}(1, 0, 0, 1), P_l = \frac{\sqrt{s}}{2}(1, 0, 0, -1) \text{ and } P_D = (E_D, P_T, 0, P_L) \quad (15)$$

where the masses of the proton and lepton have been neglected.

The gluon and the quasi-real photon carry light-cone momentum fractions $x_g = P_g^+/P_P^+$, $x_\gamma = P_\gamma^-/P_l^-$ and transverse momenta \mathbf{k}_g and \mathbf{k}_γ respectively. Their momenta are given by,

$$\begin{aligned} P_g &= x_g \frac{\sqrt{s}}{2} \left(1 + \frac{k_{\perp g}^2}{x_g^2 s}, \frac{2k_{\perp g}}{x_g \sqrt{s}} \cos \phi_{\perp g}, \frac{2k_{\perp g}}{x_g \sqrt{s}} \sin \phi_{\perp g}, 1 - \frac{k_{\perp g}^2}{x_g^2 s} \right) \\ P_\gamma &= x_\gamma \frac{\sqrt{s}}{2} \left(1 + \frac{k_{\perp \gamma}^2}{x_\gamma^2 s}, \frac{2k_{\perp \gamma}}{x_\gamma \sqrt{s}} \cos \phi_{\perp \gamma}, \frac{2k_{\perp \gamma}}{x_\gamma \sqrt{s}} \sin \phi_{\perp \gamma}, -1 + \frac{k_{\perp \gamma}^2}{x_\gamma^2 s} \right) \end{aligned} \quad (16)$$

where $\phi_{\perp g}$ and $\phi_{\perp \gamma}$ are the azimuthal angles of gluon and photon transverse momenta.

The heavy quark is produced through photon-gluon fusion $g\gamma \rightarrow c\bar{c}$ and then fragments into the heavy meson. The momentum of the heavy quark is described by z , the light-cone momentum fraction of the heavy meson and \mathbf{k}_D , the transverse momentum of the meson with respect to direction of heavy quark. In a choice of coordinates where the heavy quark momentum, \mathbf{p}_c is along the z -axis, the D -meson momentum can be written as

$$\mathbf{P}_D = (E_D, 0, 0, |\mathbf{p}_D - \mathbf{k}_D|) + (0, \mathbf{k}_D) \quad (17)$$

where the first term on the right is the component along the heavy quark direction and the second term is the component transverse to it. Here, \mathbf{k}_D is simply $(k_{D_x}, k_{D_y}, 0) = (\mathbf{k}_{D_\perp}, 0)$. In the lab coordinates however, \mathbf{k}_D can have all three components non-zero and is specified as,

$$\mathbf{k}_D = k_D (\sin \theta \cos \phi, \sin \theta \sin \phi, \cos \theta), \text{ with } |\mathbf{k}_D| = |\mathbf{k}_{D_\perp}| \quad (18)$$

and the orthogonality condition $\mathbf{k}_D \cdot \mathbf{p}_c = 0$ ensures that \mathbf{k}_D lies in a plane perpendicular to \mathbf{p}_c . The light-cone momentum fraction z is given by,

$$z = \frac{P_D^+}{P_c^+} = \frac{E_D + |\mathbf{p}_D - \mathbf{k}_D|}{E_c + |\mathbf{p}_c|} = \frac{E_D + \sqrt{\mathbf{p}_D^2 - \mathbf{k}_D^2}}{E_c + \sqrt{E_c^2 - m_c^2}} \quad (19)$$

This gives us the expression for the energy of the heavy quark,

$$E_c = \frac{m_c^2 + \left((E_D + \sqrt{\mathbf{p}_D^2 - \mathbf{k}_D^2})/z \right)^2}{2 \left((E_D + \sqrt{\mathbf{p}_D^2 - \mathbf{k}_D^2})/z \right)}. \quad (20)$$

The expression for \mathbf{p}_c can be obtained from the fact that it is collinear with $\mathbf{p}_D - \mathbf{k}_D$ and that the unit vector constructed out of both must therefore be equal,

$$\mathbf{p}_c = \sqrt{E_c^2 - m_c^2} \frac{\mathbf{p}_D - \mathbf{k}_D}{|\mathbf{p}_D - \mathbf{k}_D|}. \quad (21)$$

Eqs. 20 and 21 relate the energy and momentum of the observed D -meson with that of the fragmenting heavy quark for given values of k_D and z .

The term $d^3\mathbf{k}_D \delta(\mathbf{k}_D \cdot \hat{\mathbf{p}}_c)$ in Eqs. (2) and (3) ensures that the \mathbf{k}_D integration is only over momenta transverse to the fragmenting parton:

$$d^2\mathbf{k}_{D\perp} = d^3\mathbf{k}_D \delta(\mathbf{k}_D \cdot \hat{\mathbf{p}}_c) = dk_D k_D d\theta d\phi \frac{|\mathbf{p}_D - \mathbf{k}_D|}{P_T \sin \theta \sin \phi_1} [\delta(\phi - \phi_1) + \delta(\phi - (2\pi - \phi_1))] \quad (22)$$

where,

$$\cos \phi_1 = \frac{k_D - P_L \cos \theta}{P_T \sin \theta} \quad (23)$$

Limits on k_D can be obtained by requiring $|\cos \phi_1| \leq 1$,

$$\min [P_L \cos \theta - P_T \sin \theta, 0] \leq k_D \leq \min [P_L \cos \theta + P_T \sin \theta, 0]. \quad (24)$$

Furthermore, the inclusion of intrinsic transverse momenta in the kinematics calls for the following constraints: a) the energy of the incoming parton should not be greater than that of its parent particle, $E_{g(\gamma)} \leq E_{p(l)}$ and, b) the energy of the D -meson should not be greater than the energy of the heavy quark $E_D \leq E_c$. The first leads to the following bound on the transverse momenta of the incoming partons,

$$k_{\perp g(\gamma)} < \sqrt{s} \min[x_{g(\gamma)}, \sqrt{x_{g(\gamma)}(1 - x_{g(\gamma)})}]. \quad (25)$$

The second constraint, $E_D \leq E_c$ is inherently fulfilled by Eq. 20. However, this alone does not ensure that the heavy quark is more energetic than the D -meson in the photon-gluon c.o.m frame. By demanding $E_c > E_D$ in the $\gamma-g$ c.o.m frame, we get a lower bound on \hat{s} ,

$$\hat{s} \geq 2P_D \cdot (P_\gamma + P_g). \quad (26)$$

In our earlier work on open charm production (Ref. [20]) we had not implemented this bound in our calculations. We find that the inclusion of this bound significantly improves the convergence of the integral in the close vicinity of $x_F = 0$.

[1] L. Dick et al., Phys. Lett. **57B**, 93 (1975).

[2] R. D. Klem, J. E. Bowers, H. W. Courant, H. Kagan, M. L. Marshak, E. A. Peterson, K. Rudick, W. H. Dragoset, and J. B. Roberts, Phys. Rev. Lett. **36**, 929 (1976).

- [3] W. H. Dragoset, J. B. Roberts, J. E. Bowers, H. W. Courant, H. Kagan, M. L. Marshak, E. A. Peterson, K. Ruddick, and R. D. Klem, Phys. Rev. **D18**, 3939 (1978).
- [4] U. D'Alesio and F. Murgia, Prog. Part. Nucl. Phys. **61**, 394 (2008), 0712.4328.
- [5] V. Barone, F. Bradamante, and A. Martin, Prog. Part. Nucl. Phys. **65**, 267 (2010), 1011.0909.
- [6] U. D'Alesio and F. Murgia, Phys. Rev. **D70**, 074009 (2004), hep-ph/0408092.
- [7] D. W. Sivers, Phys. Rev. **D41**, 83 (1990).
- [8] D. W. Sivers, Phys. Rev. **D43**, 261 (1991).
- [9] U. D'Alesio, F. Murgia, and C. Pisano, JHEP **09**, 119 (2015), 1506.03078.
- [10] C. Adolph et al. (COMPASS), Phys. Lett. **B772**, 854 (2017), 1701.02453.
- [11] M. Anselmino, M. Boglione, U. D'Alesio, E. Leader, and F. Murgia, Phys. Rev. **D70**, 074025 (2004), hep-ph/0407100.
- [12] R. M. Godbole, A. Misra, A. Mukherjee, and V. S. Rawoot, Phys. Rev. **D85**, 094013 (2012), 1201.1066.
- [13] R. M. Godbole, A. Misra, A. Mukherjee, and V. S. Rawoot, Phys. Rev. **D88**, 014029 (2013), 1304.2584.
- [14] R. M. Godbole, A. Kaushik, A. Misra, and V. S. Rawoot, Phys. Rev. **D91**, 014005 (2015), 1405.3560.
- [15] U. D'Alesio, C. Flore, and F. Murgia, Phys. Rev. **D95**, 094002 (2017), 1701.01148.
- [16] U. D'Alesio, C. Flore, and F. Murgia, PoS **QCDEV2016**, 002 (2017), 1701.03303.
- [17] F. Yuan, Phys. Rev. **D78**, 014024 (2008), 0801.4357.
- [18] A. Accardi et al., Eur. Phys. J. **A52**, 268 (2016), 1212.1701.
- [19] J. Babcock, D. W. Sivers, and S. Wolfram, Phys. Rev. **D18**, 162 (1978).
- [20] R. M. Godbole, A. Kaushik, and A. Misra, Phys. Rev. **D94**, 114022 (2016), 1606.01818.
- [21] S. J. Brodsky, T. Kinoshita, and H. Terazawa, Phys. Rev. **D4**, 1532 (1971).
- [22] H. Terazawa, Rev. Mod. Phys. **45**, 615 (1973).
- [23] B. A. Kniehl, Phys. Lett. **B254**, 267 (1991).
- [24] A. Bacchetta, L. Mantovani, and B. Pasquini, Phys. Rev. **D93**, 013005 (2016), 1508.06964.
- [25] U. D'Alesio, F. Murgia, and C. Pisano, Phys. Rev. **D83**, 034021 (2011), 1011.2692.
- [26] M. Anselmino, M. Boglione, U. D'Alesio, A. Kotzinian, F. Murgia, and A. Prokudin, Phys. Rev. **D72**, 094007 (2005), [Erratum: Phys. Rev. D72, 099903 (2005)], hep-ph/0507181.
- [27] S. Kretzer, Phys. Rev. **D62**, 054001 (2000), hep-ph/0003177.

- [28] M. Anselmino, M. Boglione, U. D'Alesio, A. Kotzinian, S. Melis, F. Murgia, A. Prokudin, and C. Turk, Eur. Phys. J. **A39**, 89 (2009), 0805.2677.
- [29] D. de Florian, R. Sassot, and M. Stratmann, Phys. Rev. **D75**, 114010 (2007), hep-ph/0703242.
- [30] B. A. Kniehl and G. Kramer, Phys. Rev. **D74**, 037502 (2006), hep-ph/0607306.
- [31] A. Adare et al. (PHENIX) (2014), 1402.1209.
- [32] R. P. Feynman, R. D. Field, and G. C. Fox, Nucl. Phys. **B128**, 1 (1977).
- [33] A. P. Contogouris, R. Gaskell, and S. Papadopoulos, Phys. Rev. **D17**, 2314 (1978).